One-pot synthesis and characterization of novel boronates for the growth of single crystals with nonlinear optical properties

ARTICLE *in* DYES AND PIGMENTS · SEPTEMBER 2010

Impact Factor: 3.97 · DOI: 10.1016/j.dyepig.2010.02.007

Dyes and Pigments 87 (2010) 76–83

Contents lists available at ScienceDirect

Dyes and Pigments

journal homepage: www.elsevier.com/locate/dyepig

One-pot synthesis and characterization of novel boronates for the growth of single crystals with nonlinear optical properties

Mario Rodríguez [a], Gabriel Ramos-Ortíz [a,*], Martha I. Alcalá-Salas [a], José Luis Maldonado [a], Karla A. López-Varela [a], Yliana López [b], Oscar Domínguez [b], Marco A. Meneses-Nava [a], Oracio Barbosa-García [a], Rosa Santillan [b,*], Norberto Farfán [c]

[a] Centro de Investigaciones en Óptica, A.P. 1-948, 37000 León, Gto., Mexico
[b] Departamento de Química, Centro de Investigación y de Estudios Avanzados del IPN, 07000, Apdo. Postal. 14-740, México D. F., Mexico
[c] Facultad de Química, Departamento de Química Orgánica, Universidad Nacional Autónoma de México, México D.F. 04510, Mexico

ARTICLE INFO

Article history:
Received 18 January 2010
Received in revised form
17 February 2010
Accepted 23 February 2010
Available online 4 March 2010

Keywords:
Organic materials
Boronates
Nanomaterials
Nonlinear optics

ABSTRACT

Novel boronates were synthesized by the single step reaction of 2,4-pentanedione, aminophenol and phenylboronic acid in good yield. X-ray diffraction analysis showed that the compounds crystallized in noncentrosymmetric space groups, which was used for the growth of organic crystals with luminescent and nonlinear optical properties. For some boronates it was possible to obtain mm scale single crystals which displayed good transparency from 550 to 1200 nm. These crystals exhibited efficient second-order nonlinearity (second-harmonic generation) and third-order nonlinearity (two-photon excited fluorescence). In the case of second-harmonic generation, the observed effect was four times larger than that generated by urea which was used as a reference. Additionally, the crystals were used to prepare aqueous colloidal nanocrystals that exhibited superior fluorescence properties than those of the boronates when dissolved in organic solvents. Finally, the thermal stability of single crystals was determined using TG and TGA.

1. Introduction

In recent years, organic noncentrosymmetric materials have received considerable attention due to potential applications in nonlinear optics (NLO) namely, electro-optic light modulation, frequency conversion, parametric light generation and terahertz (THz) wave generation [1–3]. The use of organic molecules and metal-organic coordination networks as main construction blocks offer synthetic flexibility in terms of the design of novel materials that display levels of optical nonlinearity which, in many cases, are larger than those of inorganic materials. In addition, the nonlinear optical response of such compounds is of electronic origin which is of interest for the development of high-bit-rate devices.

The development of discrete organic molecules combined with various strategies to produce noncentrosymmetric packing, via the use of chiral fragments [4] and others as halogen hydrogen bonding [5], meta substitution [6], diminution of dipole moment [7] etc., have generated many organic noncentrosymmetric crystals. However, to the best of our knowledge, reports are not available on the growth and characterization of the luminescent and nonlinear optical properties of noncentrosymmetric organic crystals based on boron-containing molecules. This contrasts with the fact that in the field of nonlinear optics, boron has been extensively used for the growth of inorganic crystals, such as the series of nonlinear borate crystals: β-BaB_2O_4 (BBO), LiB_3O_5 (LBO), BiB_3O_6 (BiBO), Nd:YAl_3–$(BO_3)_4$ (NYAB), etc. [8]. In these inorganic crystals, boron is used because of its ability to coordinate with either three or four oxygen atoms, this being advantageous in the formation of structural units comprising several differental B*x*O*y* groups. This structural versatility of boron has been exploited in the growth of inorganic crystals of large effective nonlinear coefficient, wide transparency range, high damage threshold and good mechanical properties [8,9].

On the other hand, in organic synthesis, boron complexes have resulted in compounds with interesting nonlinear optical response [10] and electronic properties [11]. For instance, three-coordinated boron species have received considerable attention due to the fact that their vacant p-orbitals are strong π-electron acceptors which can lead to significant electronic delocalization within adjacent organic conjugated systems, which, in turn, results in high nonlinearity [10c]. Four-coordinated boron has also been incorporated into NLO organic systems and it was demonstrated that the

* Corresponding authors.
E-mail addresses: garamoso@cio.mx (G. Ramos-Ortíz), rsantill@cinvestav.mx (R. Santillan).

0143-7208/$ – see front matter © 2010 Elsevier Ltd. All rights reserved.
doi:10.1016/j.dyepig.2010.02.007

second-order NLO character of these boron complexes was enhanced with respect to their corresponding boron-free counterparts [12]. The present research group has studied both the second- and third- order nonlinearity of four-coordinated boron systems prepared from tridentate ligands [13,14]; these studies showed that the appropriate combination of groups (donor-acceptor) and the formation of the N → B coordinative bond optimize quadratic nonlinear effects such as the second-harmonic generation.

This work concerns the one-step synthesis of a novel series of boronates (**1a**–**1d**) as well as mm scale crystal growth from these boron complexes. This new series of boronates are interesting since the crystal packing of some of them resulted in non-centrosymmetric solids. Photoluminescence and nonlinear optical properties of these crystals are reported.

2. Experimental

2.1. Instrument

All starting materials were purchased from Aldrich. Solvents were used without further purification. Melting points were recorded on an Electrothermal 9200 apparatus and are uncorrected. Infrared spectra were measured on FT-IR Perkin–Elmer GX spectrophotometer using KBr pellets. ^{1}H, ^{11}B and ^{13}C NMR spectra were recorded on Bruker avance DPX 300 and Jeol Eclipse +400 spectrometers. Chemical shifts (ppm) are relative to $(CH_3)_4Si$ for ^{1}H and ^{13}C and to $BF_3(OEt_2)$ for ^{11}B. Ultraviolet spectra were obtained with a Perkin Elmer Lambda 12 spectrophotometer. Mass spectra were recorded on a Hewlett Packard 5989A spectrometer. Elemental analyses were carried out on a Thermo Finnigan Flash EA 1112 elemental microanalyzer.

2.2. X-ray data collection and structure determination

In all cases the single crystals suitable for X-ray structural studies were obtained by slow evaporation from mixtures of $CHCl_3$ or CH_2Cl_2. The crystal data were recorded on an Enraf Nonius Kappa-CCD (λ MoKα = 0.71073 Å, graphite monochromator, $T = 293$ K-CCD). The crystals were mounted on a Lindeman tube. All reflection data set were corrected for Lorentz and polarization effects. The first structure solution was obtained using the SHELXS-97 and SIR2004 programs and then the SHELXL-97 programs was applied for refinement and output data. All software manipulations were done under the WinGX environment program set [15]. Molecular perspectives were drawn under DIAMOND drawing application. All heavier atoms were found by Fourier map difference and refined anisotropically. The hydrogen atoms were geometrically modelled and are not refined.

2.3. Synthesis

The following procedure was employed in the preparation of all boron compounds described herein. Equimolar amounts of aminophenol, 2,4-pentanedione and phenylboronic acid were placed in a flask to which was added 20 mL of benzene and the ensuing solution was refluxed for 2h. Excess solvent was eliminated with a Dean–Stark trap and the solid precipitate was collected by filtration under vacuum and washed with hexane (see Scheme. 1).

2.3.1. 8,10-Dimethyl-6-phenyl-5,7-dioxa-11-aza-6-bora-benzocyclononene (*1a*)

Compound **1a** was prepared from the reaction of 2-aminophenol 1.00 g (9.9 mmol), 2,4-pentanedione 1.00 g (9.9 mmol) and phenylboronic acid 1.20 g (9.9 mmol), to give 2.20 g (8.2 mmol, 80% yield) of **1a** as a yellow solid. M.P.: 149–150 °C. IR_{vmax} (KBr): 3003, 1596, 1513, 1387, 1307, 1285, 1250, 1175, 1116, 1022, 957 cm^{-1}. ^{1}H NMR (300 MHz, $CDCl_3$) δ: 2.25 (3H, s, H-1), 2.45 (3H, s, H-5), 5.57 (1H, s H-3), 6.84 (1H, t, $J = 8.0$ Hz, H-9), 7.04 (1H, dd, $J = 8.1$, 1.0 Hz, H-7), 7.20 (1H, t, $J = 8.1$ Hz, H-8), 7.21–7.24 (3H, m, H-*m*, *p*), 7.34 (1H, d, $J = 7.8$ Hz, H-10), 7.36–7.38 (2H, m, H-*o*) ppm. ^{13}C NMR (75 MHz, $CDCl_3$) δ: 21.3 (C-1), 22.9 (C-5) 103.6 (C-3), 114.1 (C-7), 117.9 (C-10), 118.7 (C-9), 127.4 (C-*m*), 127.7 (C-*p*), 128.9 (C-8), 130.9 (C-*o*), 132.5 (C-6), 156.8 (C-11), 161.2 (C-2), 173.3 (C-4) ppm. ^{11}B-NMR (96 MHz, $CDCl_3$) δ: 7.9 ppm. EM (20 eV) *m*/*z* (%): 277 (M^+, 0.3), 201 (9), 200 ($M^+ - C_6H_5$, 100), 199 (26), 185 (10), 77 (8), 43 (5). Anal. Calc. for $C_{17}H_{16}BNO_2$; C, 74.25; H, 6.23; N, 4.81. Found: C, 74.32; H, 6.49; N, 4.83.

2.3.2. 2-Chloro-8,10-dimethyl-6-phenyl-5,7-dioxa-11-aza-6-bora-benzocyclononene (*1b*)

Compound **1b** was prepared from the reaction of 2-amino-4-chlorophenol 1.40 g (9.9 mmol), 2,4-pentanedione 1.00 g (9.9 mmol) and phenylboronic acid 1.20 g (9.9 mmol), to give 2.80 g (9.0 mmol, 90% yield) of **1b** as a yellow solid. M.P.: 137–138 °C. IR_{vmax} (KBr): 3009, 1615, 1518, 1473, 1430, 1317, 1258, 1180, 1125, 943 cm^{-1}. ^{1}H NMR (400 MHz, $CDCl_3$) δ: 2.24 (3H, s, H-1), 2.44 (3H, s, H-5), 5.60 (1H, s H-3), 6.94 (1H, d, $J = 8.8$ Hz,H-10), 7.15 (1H, dd, $J = 8.5$, 2.2 Hz, H-9), 7.30 (1H, s, H-7), 7.20–7.31 (3H, m, H-*m*, *p*), 7.29-7-31 (2H, m, H-*o*) ppm. ^{13}C NMR (100 MHz, $CDCl_3$) δ: 21.3 (C-1), 23.1 (C-5) 103.9 (C-3), 114.6 (C-10), 118.0 (C-7), 123.1 (C-8), 127.5 (C-*m*), 127.9 (C-*p*), 128.5 (C-9), 130.8 (C-*o*), 133.1 (C-6), 155.3 (C-11), 162.0 (C-2), 174.5 (C-4) ppm. ^{11}B NMR (128 MHz, $CDCl_3$) δ: 8.1 ppm. EM (20 eV) *m*/*z* (%): 313 (M^+, 1), 311 (3), 236 ($M^+ - C_6H_5$, 50), 234 ($M^+ - C_6H_5$, 100), 219 (2), 199 (21), 77 (1), 43 (3). Anal. Calc. for $C_{17}H_{15}BNO_2Cl$; C, 65.53; H, 4.85; N, 4.50. Found: C, 65.28; H, 4.95; N, 4.49.

2.3.3. 2-Methyl-8,10-dimethyl-6-phenyl-5,7-dioxa-11-aza-6-bora-benzocyclononene (*1c*)

Compound **1c** was prepared from the reaction of 2-amino-4-methylphenol 1.20 g (9.9 mmol), 2,4-pentanedione 1.00 g (9.9 mmol) and phenylboronic acid 1.20 g (9.9 mmol), to give 2.80 g (9.6 mmol, 97% yield) of **1c** as a yellow solid. M.P.: 120–121 °C. IR_{vmax} (KBr): 3006, 2916, 1618, 1587, 1521, 1365, 1310, 1430, 1178, 1128, 946 cm^{-1} ^{1}H NMR (300 MHz, $CDCl_3$) δ: 2.22 (3H, s, H-1), 2.33 (3H, s, Me), 2.43 (3H, s, H-5), 5.53 (1H, s, H-3), 6.93 (1H, d, $J = 8.1$ Hz, H-10), 6.99 (1H, dd, $J = 8.3$ Hz, H-9), 7.15 (1H, s, H-7), 7.21-7-22 (2H, m, H-*o*) 7.33–7.35 (3H, m, H-*m*, *p*) ppm. ^{13}C NMR (75 MHz, $CDCl_3$) δ: 21.3 (C-1), 21.3 (C-12), 22.9 (C-5), 103.5 (C-3), 113.6 (C-10), 118.5 (C-7), 127.4 (C-9), 127.66 (C-*m*), 128.0 (C-*p*), 129.4 (C-8), 130.9 (C-*o*), 132.3 (C-6), 154.6 (C-11), 160.7 (C-2), 173.0 (C-4) ppm. ^{11}B-NMR (96 MHz, $CDCl_3$) δ: 7.8 ppm. EM (20 eV) *m*/*z* (%): 291 (M^+, 4), 215 (13), 214 ($M^+ - C_6H_5$, 100), 199 (3). Anal. Calc. for $C_{18}H_{18}BNO_2$; C, 74.25; H, 6.23; N, 4.81. Found: C, 74.32; H, 6.69; N, 4.83.

2.3.4. 2-Nitro-8,10-dimethyl-6-phenyl-5,7-dioxa-11-aza-6-bora-benzocyclononene (*1d*)

Compound **1d** was prepared from the reaction of 2-amino-4-nitrophenol 1.50 g (9.9 mmol), 2,4-pentanedione 1.00 g (9.9 mmol) and phenylboronic acid 1.20 g (9.9 mmol), to give 2.60 g (8.0 mmol, 80% yield) of **1d** as a green solid. M.P.: 178–179 °C. IR_{vmax} (KBr): 3009, 1610, 1511, 1433, 1387, 1368, 1336, 1311, 1280, 1186, 927, 888, 753, 705 cm^{-1}, ^{1}H NMR (300 MHz, $CDCl_3$) δ: 2.30 (3H, s, H-1), 2.57 (3H, s, H-5), 5.72 (1H, s, H-3), 7.06 (1H, d, $J = 8.8$ Hz, H-10), 7.21–7.32 (5H, m, H-*o*, *m*, *p*), 8.20 (1H, d, $J = 2.4$ Hz, H-7), 8.24 (1H, dd, $J = 8.8$, 2.4 Hz, H-9) ppm. ^{13}C NMR (75 MHz, $CDCl_3$) δ: 21.8 (C-1), 23.5 (C-5), 104.7 (C-3), 113.4 (C-10), 114.0 (C-9), 126.1 (C-7), 127.9 (C-*m*), 128.6 (C-*p*), 131.0 (C-*o*), 132.7 (C-6), 140.0 (C-8), 162.5 (C-11), 164.1 (C-2), 176.4 (C-4) ppm. ^{11}B NMR (96 MHz, $CDCl_3$) δ: 8.8 ppm. EM (20 eV) *m*/*z* (%): 322 (M^+,2), 318 (56), 317 (27), 215 (14), 214 (100), 213 (33), 128 (10). Anal. Calc. for $C_{17}H_{15}BN_2O_4$: C; 63.39. H; 4.69, N; 8.70, Found: C; 63.39. H; 5.08, N; 8.83.

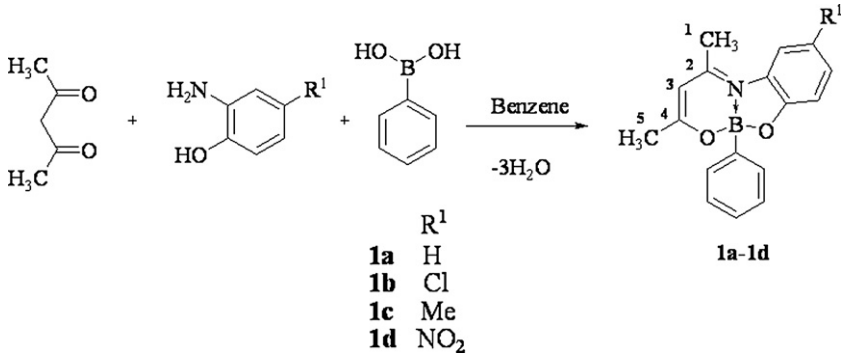

Scheme 1. Synthesis of boronates **1a**–**1d** in one step from the reaction of 2,4-pentanedione, aminophenol and phenylboronic acid.

CCDC 758819 (**1a**), 758820 (**1b**) and 758821 (**1c**) contain the supplementary crystallographic data for this paper. These data can be obtained free of charge from The Cambridge Crystallographic Data Centre via www.ccdc.cam.ac.uk/data_request/cif.

3. Results and discussion

3.1. Synthesis and spectroscopic characterization of the boron complexes *1a*–*1d*

The series of boronates **1a**–**1d** were prepared from the reaction in one step of 2,4-pentanedione, aminophenol and phenylboronic acid, at reflux of benzene for 2 h (see Scheme. 1). These new [4.3.0] heterobicyclic boronates were obtained in good yields, as colored solids which are soluble in common organic solvents. The molecules were re-crystallized several times in dichloromethane to perform the physical and chemical analysis. As a first insight into the formation of compounds **1a**–**1d** the IR spectral analysis showed stretching bands from 1511 to 1521 cm^{-1} which are assigned to the C=N bond and from 1587 to 1615 cm^{-1} assigned to the C=C double bond. In general, the mass spectra of boronates show the peak for the molecular ion and the base peak corresponding to loss of the arylboronic fragment [14].

The analysis of the spectroscopic data established the formation of **1a**–**1d** (Table 1). The ^{1}H NMR spectra for these new boronates showed signals for two different methyl groups H-1 and H-5 in 2.22–2.30 and 2.43–2.57 ppm, respectively. Furthermore, the signal for H-3 presents a chemical shift from 5.53 to 5.72 ppm that evidences the presence of *enol-imine* tautomer in the boronate structure. The ^{1}H signals corresponding to the aromatic part of the molecule were assigned based on the coupling constant values and with the ^{1}H-^{1}H COSY NMR technique. The ^{13}C NMR spectra of boronates **1a**–**1d** showed two methyl signals with a chemical shift of 21.3–22.0 and 22.9–23.7 ppm corresponding to C-1 and C-5, respectively. On the other hand, the signal corresponding to the iminic carbon appears from 160.7 to 164.1 ppm and the C-4 base enol moiety from 173.0 to 176.4 ppm. All signals of the ^{13}C NMR spectra were assigned employing ^{1}H–^{13}C HETCOR and HMBC NMR technique. Finally, the ^{11}B NMR analysis of compounds **1a**–**1d** confirmed the presence of tetra-coordinate boron atom for the observed chemical shift between 7.8 and 8.8 ppm.

Table 1
NMR Chemical shifts for compounds **1a**–**1d** obtained in a Bruker avance DPX 300 spectrometer in $CDCl_3$ as a solvent.

	NMR shifts (ppm)							IR (cm^{-1})	
	H-1	H-3	H-5	C-2	C-3	C-4	^{11}B	C=C	C=N
1a	2.25	5.57	2.45	161.2	103.6	173.3	7.9	1596	1513
1b	2.24	5.60	2.44	162.0	103.9	174.5	8.1	1615	1518
1c	2.22	5.53	2.43	160.7	103.5	173.0	7.8	1587	1521
1d	2.30	5.72	2.57	164.1	104.7	176.4	8.8	1610	1511

3.2. X-ray analysis

The crystals for X-ray diffraction analysis were obtained by slow evaporation of concentrated solutions of each boronate (**1a**–**1d**) in dichloromethane or ethyl acetate at room temperature. For compounds **1a**, **1b** and **1d** it was possible to obtain crystals suitable for X-ray diffraction. A summary of selected angles, bond distances and torsion angles are contained in Table 2. The X-ray diffraction analysis confirmed the structure of the boronates containing a tetra-coordinated boron atom (Fig. 1), with three covalent bonds (two B–O bonds and one B–C bond) and additionally a coordinative N → B bond with a length of 1.575(3), 1.577(2) and 1.5768(19) Å for **1a**, **1b** and **1d**, respectively. The values for the coordinative bond lengths are shorter than the values shown by boronates assembled from salicylidenimino alcohol ligands (from 1.586(2) to 1.861(5) Å) [14,16], but they are similar to those reported for boronates prepared from the reaction of a ketoenamine ligand with two units

Table 2
Selected bond lengths (Å), angles (°) and torsion angles (°) for boronates **1a**, **1b** and **1d**.

Compounds	1a	1b	1d
N(1)–B(1)	1.575 (3)	1.577 (2)	1.5768 (17)
N(1)–C(6)	1.413 (3)	1.4121 (19)	1.4104 (17)
N(1)–C(2)	1.313 (3)	1.314 (3)	1.3162 (17)
C(2)–C(3)	1.421 (3)	1.418 (3)	1.421 (2)
C(3)–C(4)	1.360 (4)	1.360 (3)	1.367 (2)
C(4)–C(5)	1.484 (4)	1.321 (3)	1.493 (2)
C(4)–O(1)	1.326 (3)	1.321 (3)	1.3259 (19)
B(1)–O(1)	1.476 (3)	1.479 (2)	1.4735 (19)
B(1)–O(2)	1.481 (3)	1.488 (2)	1.4992 (19)
B(1)–C_{Ph}	1.602 (3)	1.610 (2)	1.607 (2)
O(1)–B(1)–N(1)	107.32 (17)	107.68 (12)	107.94 (10)
O(1)–B(1)–O(2)	111.73 (18)	111.63 (13)	111.31 (12)
O(1)–B(1)–C_{Ph}	111.46 (19)	111.12 (13)	111.67 (12)
O(2)–B(1)–N(1)	100.79 (17)	100.88 (12)	100.18 (11)
O(2)–B(1)–C_{Ph}	112.33 (17)	112.30 (12)	111.74 (11)
N(1)–B(1)–C_{Ph}	112.67 (18)	112.75 (12)	113.44 (11)
C(2)–N(1)–B(1)	120.10 (18)	121.00 (13)	121.21 (11)
C(2)–C(3)–C(4)	120.8 (2)	120.8 (2)	120.75 (14)
N(1)–C(2)–C(3)–C(4)	−19.7 (4)	−19.93 (3)	−20.5 (2)
C(2)–C(3)–C(4)–O(1)	11.0 (4)	9.9 (3)	155.49 (15)
O(1)–B(1)–N(1)–C(2)	37.3 (3)	34.37 (19)	32.19 (17)
C(2)–N(1)–C(6)–C(7)	−160.6 (2)	25.3 (3)	29.3 (2)
N(1)–C(6)–C(7)–O(2)	1.9 (2)	−0.59 (17)	−0.04 (15)

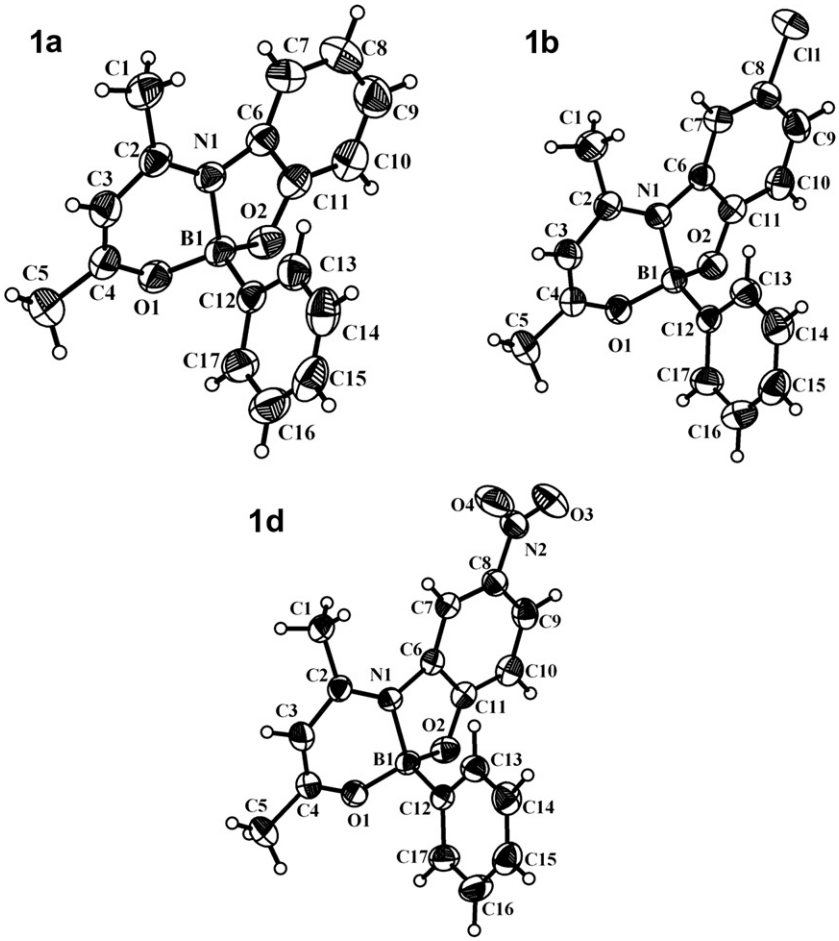

Fig. 1. Perspective views of the molecular structures of compounds **1a**, **1b** and **1d**. Their ellipsoids are shown at the 20% probability level.

of phenylboronic acid [1.574(4) Å] [17]. The analysis of the covalent B–O bond for boronates **1a**, **1b** and **1d** showed shorter bond lengths for the B–O(1) distance than the values reported previously in other boronates (1.496(6) Å) [17], indicating that the boronates reported herein exist as the enolimine tautomers.

The three boron compounds **1a**, **1b** and **1d** analyzed in this work crystallized in the space group $P\,2_12_12_1$ that belongs to the orthorhombic crystal system. The crystal features and collection data are summarized in Table 3. All crystals contain one crystallographic independent molecule in the asymmetric unit. It is worth to notice that this series of boronates crystallize in a noncentrosymmetric space group, this can be attributed to various facts including the small size of the electronic π-system, the low dipole moment value and the strong intermolecular hydrogen bond. The introduction of the B-phenyl moiety contained in compound **1a** did not affect the packing, in fact the X-ray diffraction analysis showed that its precursor ligand also crystallizes in a noncentrosymmetric space group ($P\,2_12_12_1$) [18a]; in the case of the ligand **1b** the crystallization occurs in the space group $P\,2_1/a$, but the addition of the B-phenyl group favored the crystallization in the noncentrosymmetric space group $P\,2_12_12_1$ [18b].

The supramolecular analysis for **1a**, **1b** and **1d** shows that the stabilization of the crystal structure is due to non classical hydrogen bonds. In the case of compound **1b** that contains a chlorine atom, this promotes strong C(13)–H(13)···Cl^i(1) interactions ($i = -1/2 + x, 3/2 - y, -z$) with a C(13)···Cl(1) distance of 3.6347(19) Å and an angle of 137.25(12)°. The expansion of the previous interaction leads to the formation of molecular chains containing molecules related by screw axis (Fig. 2).

3.3. Growth of single crystals

The crystals of compounds **1b** and **1d** were grown further to larger size by using conventional crystal growth techniques. A saturated solution of **1b** and **1d** (0.5 g) in chloroform (3 mL) was

Table 3
Crystal data for boronates **1a**, **1b** and **1d**.

Compound	**1a**	**1b**	**1d**
Chemical formula	$C_{17}H_{16}BNO_2$	$C_{17}H_{15}BClNO_2$	$C_{17}H_{15}BN_2O_4$
Mol wt.	277.12	311.58	322.12
Space group	$P\,2_12_12_1$	$P\,2_12_12_1$	$P\,2_12_12_1$
a (Å)	8.4610 (1)	8.4550 (1)	8.5364 (2)
b (Å)	11.554 (2)	12.5096 (2)	12.5227 (6)
c (Å)	14.889 (3)	14.4744 (3)	14.4121 (3)
α (o)	90	90	90
β (o)	90	90	90
γ (o)	90	90	90
V (Å^{-3})	1455.5 (4)	1531.48	1541.70
Z	4	4	4
$\rho_{calcd.}$ (g/cm^3)	1.265	1.351	1.388
Θ Range (°)	3–27	4–27	3–27
No. of reflections			
Measured	6558	3462	8587
Unique	1879	3462	3273
Observed	1512	3092	2984
R [$I > 2\sigma(I)$]	0.0376	0.0364	0.0374
Rw (all data)	0.0977	0.0882	0.0991
Parameters	204	201	251
ρ_{min} (e Å^{-3})	−0.197	−0.213	−0.127
ρ_{max} (e Å^{-3})	0.216	0.131	0.116
GOOF	1.056	1.044	1.026

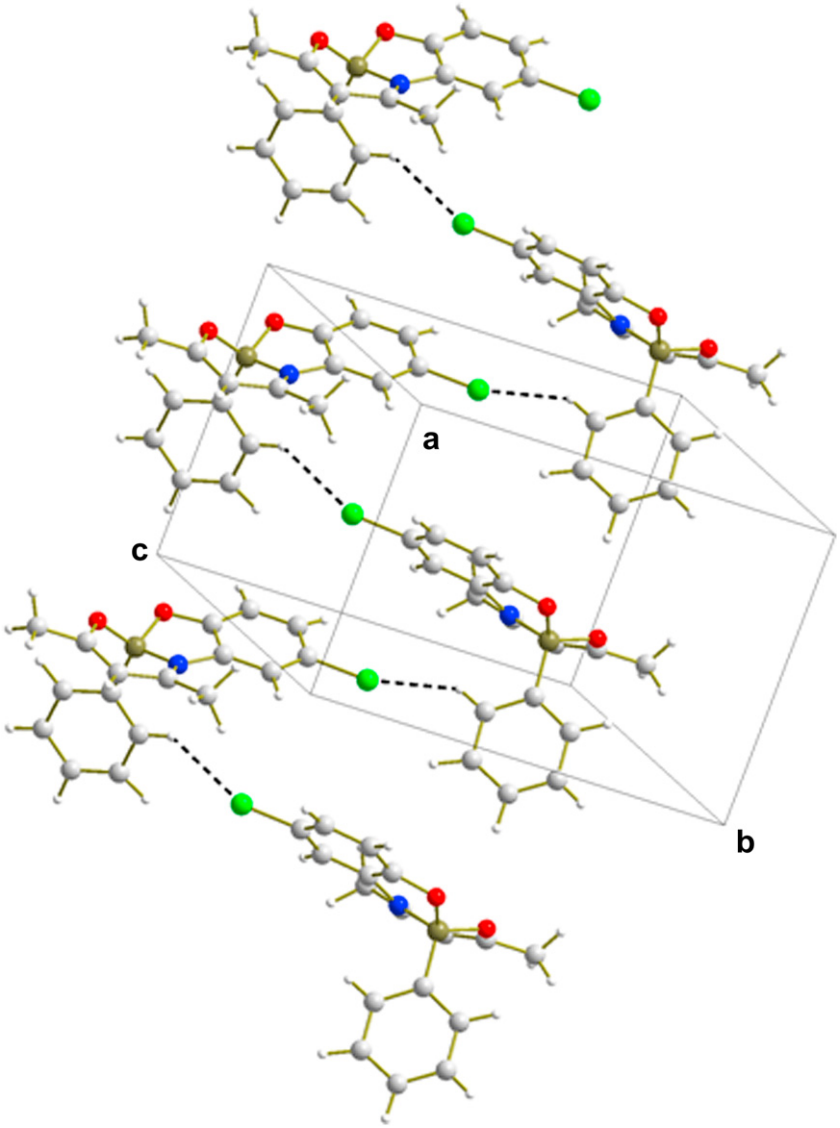

Fig. 2. Molecular interactions in the crystal of compound **1b**.

prepared. The solution was stirred at slow rate and refluxed at 77 °C for 4 h. The refluxed solution was covered and kept undisturbed for slow cooling and slow evaporation of the solvent at room temperature. Yellow-color crystals were obtained in the form of plates, needles or bulk structures after a few days. Fig. 3 shows some crystals obtained with this method.

3.4. Thermal analysis

The thermogravimetric (TG) analysis of crystals **1b** and **1d** was carried out in the temperature range from 25 to 450 °C under nitrogen atmosphere at a heating rate of 10 °C min^{-1} using a Thermobalance Mettler Toledo TGASDTA851e thermal analyzer. As an example, the thermogram for compound **1d** and its differential thermogravimetric curve are shown in Fig. 4. In this TG analysis there is no significant weight loss until 240 °C but continuous weight loss can be detected from 240 to 290 °C. At the latter temperature the weight loss is 55% and the resulting residue undergoes degradation up to 500 °C. The DTA analysis showed an endothermic peak in 245.7 °C corresponding to the melting process. Similarly, in the case of compound **1b**, the main weight loss of the crystal is detected from 220 to 260 °C. The DTA analysis for compound **1b** showed an endothermic peak in 252 °C.

3.5. Optical characterization

The UV–visible absorption spectra of the boronates **1a**, **1b**, **1c** and **1d** exhibited similar spectral features (see Fig. 5) with main peaks at 400, 407, 409 and 390 nm, respectively. For these compounds the characteristic absorption band can be assigned to a ligand-centered electronic $S_0 \rightarrow S_1$ (π–π^*) transition. The optical region of transparency for single crystals obtained from these boronates is a key feature to be examined. For instance, the transparency properties for single crystals grown from the boronates **1b** and **1d** are shown in the inset of Fig. 5. Both crystals are semi-transparent in a wide range of the visible spectrum with cutoff wavelengths at 500 and 460 nm, respectively. The small discontinuities at 860 nm observed in the spectra presented in this figure are due to a change in the spectrophotometer detector.

It is worth to mention that the boronates **1a**–**1d** exhibited very weak photoluminescence in solution. Nevertheless, the photoluminescence properties were remarkably enhanced in single

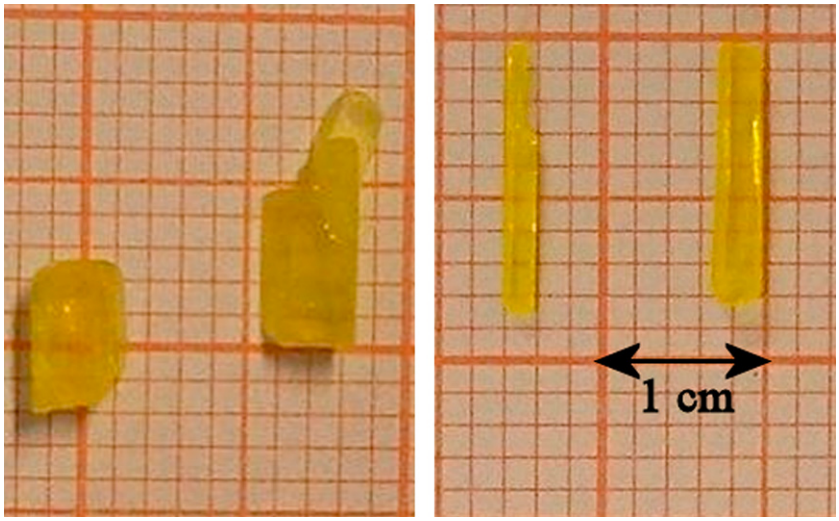

Fig. 3. Photograph of single crystals of compounds **1b** (in the left) and **1d** (in the right).

crystals. For instance, the crystals grown from the boronates **1b** and **1d** emit intense green fluorescence upon excitation at 370 nm (excitation from a UV lamp). The emission peaks for these crystals are 544 nm and 509 nm, respectively (see Fig. 6). As expected, the emission peak of crystal **1b** is red-shifted with respect to the peak corresponding to crystal **1d** since its cutoff frequency in the absorption spectrum is located at larger wavelength.

Interestingly, nanocrystals of **1b** and **1d** also exhibited strong fluorescence. For example, the inset in Fig. 6 shows the emission spectrum from a colloidal solution of nanocrystals (<200 nm in size) of **1b**; it is observed that the peak of fluorescence from these nanocrystals is blue-shifted approximately 22 nm with respect to the peak observed for the corresponding single crystal. Fig. 7 shows a photograph of the luminescence observed from the colloidal solution; for comparison, this figure also shows the absence of fluorescence from a chloroform solution of **1b** with the same molar concentration that the colloidal solution of nanocrystals. To produce these nanocrystals the laser ablation procedure [19] was employed where 0.3 mg of micrometer-sized crystals (obtained by hand-grinding single crystals **1b** or **1d**) were suspended in a poor solvent (aqueous solution of cetyl trimethyl ammonium bromide, CTAB, 0.08 mM) and then exposed to the third-harmonic beam (355 nm) of a nanosecond Nd:YAG laser (7 ns, 10 Hz repetition rate and 43 mJ/cm^2 at sample position) to produce microcrystal fragmentation. In this procedure the fragmented material is then caught by water and stabilized as nanocolloids. In order to get a homogenous ablation process, the solution was stirred vigorously using a magnetic stirrer. After the laser ablation process was completed the colloidal solution was filtered through 200 nm PTFE membrane filters.

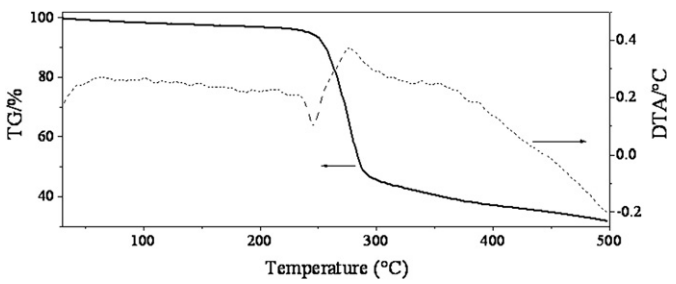

Fig. 4. TG and DTA graphs of crystal **1d**.

On the other hand, the single crystals also emitted fluorescence under multi-photon excitation. By pumping these crystals with femtosecond laser pulses (100 fs, 80 MHz repetition rate) at 800 nm, a relative intense fluorescence was seen by the naked eye in a room with normal illumination conditions. Since these crystals are transparent at 800 nm, thus it follows that the fluorescence can only occur by means of multi-photon process, i.e., two-photon absorption (TPA). This is because the two-photon energy at 800 nm falls into the one-photon absorption band of the boronates (see Fig. 5). The photoluminescence spectra of the crystals **1b** and **1d** excited by two photons (800 nm) are compared with that observed with those excited by one photon (see Fig. 6). It is observed that the spectral shape is practically the same, indicating that the light emission induced by one-photon and two-photons originates from the same excited state in the crystals.

3.6. Studies of the second-harmonic generation (SHG)

SHG measurements performed on single crystals **1b** and **1d** were performed to confirm their noncentrosymmetric structures and to evaluate their potential use as a second-order NLO materials.

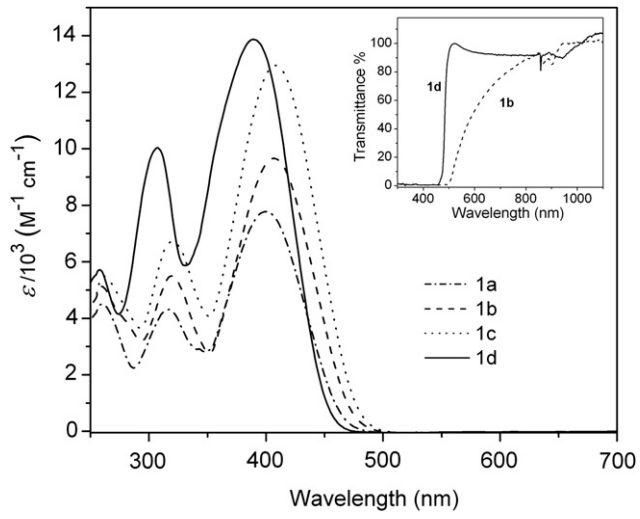

Fig. 5. UV–visible absorption spectra for boron compounds **1a**–**1d**. Inset: Transmission spectra of single crystals obtained with **1b** and **1d**.

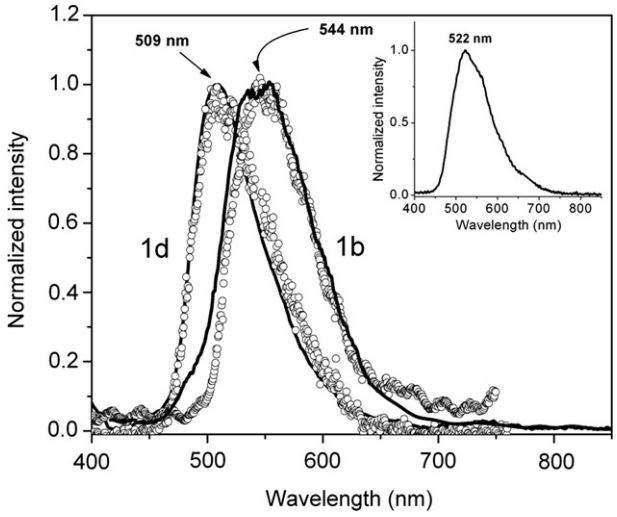

Fig. 6. Photoluminescence spectra for single crystals **1b** and **1d** obtained under one-photon excitation at 370 nm (continuous lines) and two-photon excitation at 800 nm (open circles). Inset: Photoluminescence spectrum from colloidal solution of nanocrystals of **1b** excited at 370 nm.

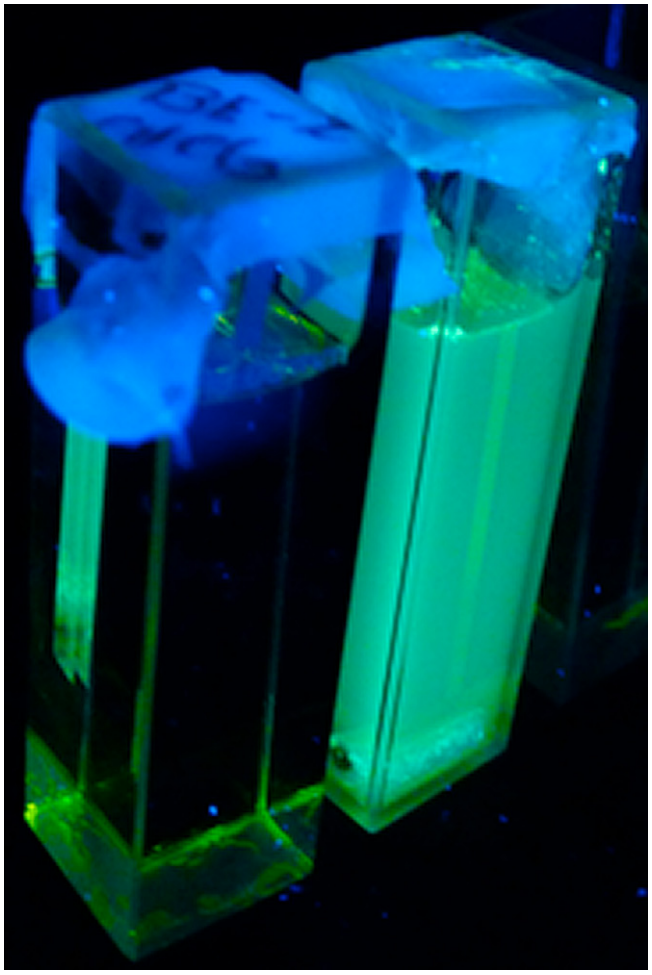

Fig. 7. Photoluminescence from boronate **1b** in a chloroform solution (left in the picture) and from a colloidal solution of nanocrystals (right in the picture). Fluorescence was obtained under excitation at 370 nm.

As excitation source, a Nd-YAG laser-pumped optical parametric oscillator (OPO) that delivered pulses of 7 ns at a repetition rate of 10 Hz was employed. When the idler beam of this OPO system was focused into the crystals (3 mJ/pulse at sample position) and the wavelength was tuned in the IR wavelength range between 1100 and 1600 nm, the SHG effect was confirmed by detecting monochromatic radiation from green (550 nm) to near IR (800 nm), respectively. It is worth to point out that at this range of wavelengths no fluorescence induced by two-photon absorption was detected, indicating that the latter effect is only efficient under excitation around 800 nm. This was expected since the absorption peaks for these materials are near 400 nm, being 800 nm the two-photon resonance wavelength as discussed before. Measurement of the SGH efficiency of **1b** and **1d** was performed by the Kurtz-Perry [20] powder technique. For the use of this technique, fine powder from the crystals was sandwiched between two glass slides. After the samples, a low pass filter was used to block IR wavelength. The SHG signal was then focused into the input slit of an imaging spectrograph and recorded at the exit with a CCD camera. Under the same experimental conditions, the SHG signal from urea was obtained. The SHG signal from the crystal of boronates **1b** and **1d** resulted in average 4 times larger than that of urea crystals at 1200 nm. By comparing the SHG capacity of urea and that of the technologically useful potassium dihydrogenphosphate (KDP) [21], revealed that single crystals grown from compounds **1b** and **1d** exhibit SHG efficiency about 26 times higher than KDP.

4. Conclusions

A new series of boronates obtained by one-pot synthesis were utilized for the growth of single crystal with the size of few millimeters. These compounds tend to crystallize in the non-centrosymmetric space group $P\,2_12_12_1$ promoted by non classical hydrogen bonds and for the small size of the main backbone. Nonlinear optical studies confirmed that the SHG efficiency of these crystals is in average 4 times larger than in urea and 26 times larger than in KDP. Further, these crystals exhibit notorious fluorescence induced by one-photon and two-photon absorption at the resonant wavelengths about 400 and 800 nm, respectively. Interestingly, the photoluminescence properties are conserved in colloidal solution of nanocrystals. This is the first report about the preparation of organic crystals in the scale of millimeters with boron derivatives and offers the opportunity to investigate other organoboron compounds in nonlinear organic crystals.

Acknowledgements

One of the authors (M. Rodríguez) thanks to CONACyT for a scholarship. This work was supported by CONACyT (Projects J49512F and 55250) and UNAM (PAPIIT IN-214010). The authors thank Martín Olmos for technical assistance, Maria Luisa Rodríguez for NMR experiments, Marco Leyva for X-ray analysis and Geiser Cuellar for MS.

References

[1] Nalwa HS, Miyata S, editors. Nonlinear optics of organic molecules and polymers. Boca Raton, FL: CRC Press; 1997.
[2] Ch Bosshard, Sutter K, Prêtre Ph, Hulliger J, Flörsheimer M, Kaatz P, et al. Organic nonlinear optical materials. Gordon and Breach; 1995.
[3] Schneider A, Neis M, Stillhart M, Ruiz B, Khan RUA, Günter P. J Opt Soc Am 1822;2006:23.
[4] (a) Nagaraja HS, Upadhyaya V, Rao PM, Aithal PS, Bhat AP. J Cryst Growth 1993;193:674;
(b) Nestorov VV, Antipin MY, Nesterov VN, Timofeeva TV. J Mol Struct 2007;831:18.

[5] (a) Babu RR, Vijayan N, Gunasekaran M, Gopalakrishnan R, Ramasamy P. J Cryst Growth 2004;265:290;
(b) Sethuraman K, Babu RR, Vijayan N, Gopalakrishnan R, Ramasamy P. Spectrochim Acta A 2007;66:707.
[6] Zyss J. J Phys D Appl Phys 1993;26:8198.
[7] Zyss J, Chemla DS, Nicoud IF. J Chem Phys 1981;74:4800.
[8] Becker P. Adv Mater 1998;10:979.
[9] Xue D, Betzler K, Hesse H, Lammers D. Solid State Commun 2000;114:21.
[10] (a) Collings JC, Poon SY, Droumaguet CL, Charlot M, Katan C, Pålsson LO, et al. Chem Eur J 2009;15:198;
(b) Yuan Z, Entwistle CD, Collings JC, Albesa-Jové D, Batsanov AS, Howard JAK, et al. Chem Eur J 2006;12:2758;
(c) Entwistle CD, Marder TB. Angew Chem Int Ed 2002;41:2927;
(d) Zhao L, Yang G, Su Z, Yan L. J Mol Struct THEOCHEM 2008;855:69;
(e) Lamère JF, Lacroix PG, Farfán N, Rivera JM, Santillan R, Nakatani K. J Mater Chem 2006;16:2913.
[11] (a) Cui Y, Li F, Lu ZH, Wang S. Dalton Trans; 2007:2634;
(b) Zhou G, Ho CL, Wong WY, Wang Q, Ma D, Wang L, et al. Adv Funct Mater 2008;18:499;
(c) Lin SL, Chan LH, Lee RH, Yen MY, Kuo WJ, Chen CT, et al. Adv Mater 2008;20:3947;
(d) Zhao SB, Wucher P, Hudson ZM, McCormick TM, Liu XY, Wang S, et al. Organometallics 2008;27:6446.
[12] (a) Lesley MJG, Woodward A, Taylor NJ, Marder TB, Cazenobe I, Ledoux I, et al. Chem Mater 1998;10:1355;
(b) Lambert C, Stadler S, Bourhill G, Brauchle C. Angew Chem Int Ed Engl 1996;35:644.
[13] Muñoz BM, Santillan R, Rodríguez M, Méndez JM, Romero M, Farfán N, et al. J Organomet Chem 2008;693:1321.
[14] Reyes H, Muñoz BM, Farfán N, Santillan R, Rojas-Lima S, Lacroix PG, et al. J Mater Chem 2002;12:2898.
[15] Sheldrick GM. SHEXL-97. Program for crystal structure solution. University of Göttingen Germany; 1997.
[16] (a) Barba V, Cuahutle D, Santillan R, Farfán N. Can J Chem 2001;79:1229;
(b) Rodríguez M, Ochoa ME, Santillán R, Farfán N, Barba V. J Organomet Chem 2005;690:2975.
[17] Sánchez M, Sánchez O, Höpfl H, Ochoa ME, Castillo D, Farfán N, et al. J Organomet Chem 2004;689:811.
[18] (a) Arici C, Nawaz M, Ülkü D, Atakol O. Acta Cryst C 1999;55:1691;
(b) Kabak M, Elmali A, Elerman Y. J Mol Struct 1998;470:295.
[19] Asahi T, Sugiyama T, Masuhara H. Acc Chem Res 2008;41:1790.
[20] Kurtz SK, Perry TA. J Appl Phys 1968;39:3798.
[21] (a) Srinivasan P, Kanagasekaran T, Gopalakrishnan R. Cryst Growth Des 2008; 8:2340;
(b) Srinivasan P, Kanagasekaran T, Gopalakrishnan R, Bhagavannarayana G, Ramasamy P. Cryst Growth Des 2006;6:1663.